To Study CFD Analysis of Heat Transfer in the Supercritical Nuclear Reactor Fuel Rod Assemblage with R-12 Coolant

Adarsh Tripathi[1] Mr. Shani Kumar[2] Mr. Sangam Kumar[3]
[1,2]M. Tech. Student [3]Assistant Professor
[1,2,3]Department of Mechanical Engineering
[1,3]Suyas Institute of information and Technology, Gorakhpur-273016, Uttar Pradesh, India [2]Madan Mohan Malaviya University of Technology, Gorakhpur-273010, Uttar Pradesh, India

Abstract— The steady state temperature distribution in a nuclear fuel rod using R-12 as coolant has been discussed in this paper. A high amount of energy is released by fission reaction within the nuclear fuel rod. This energy is then transferred by heat conduction to the surface of the fuel rod.. In this work, a model of the equivalent nuclear reactor is prepared in ANSYS design modeler and two particular sub channels are taken. The physical dimensions and the input data required during modeling as well as computation have been taken from an experimental paper; where inlet pressure is 4.63 MPa, inlet temperature is 392 K and heat flux is 33.5kW/m^2. Analysis has been done through ANSYS CFD technique to obtain steady state heat transfer in nuclear reactor fuel rod assembly and the local heat transfer coefficient of supercritical R-12 in sub channels of CANDU reactor under cooling conditions which is equivalent to a supercritical water reactor. Hence to confirm the turbulent nature of the flow, Reynolds number variation across the heated length is found out. Later; input conditions such as mass flux, heat flux, and pitch to diameter ratio and inlet pressure are varied to observe its effects on temperature distribution and local heat transfer coefficient. Hence results in the enhancement of heat transfer from the fuel rod cladding surface.

Key words: CFD, FVM and R-12 as Coolant

I. INTRODUCTION

In the nuclear physics and nuclear chemistry, a nuclear reaction is semantically measured to be the process in which two nuclei, or a nucleus of an atom and a subatomic particle such as a proton, neutron, or high energy electron from outside the atom, have a collision to produce one or more nuclei that are dissimilar from the parent nuclei. Nuclear fusion and nuclear fission are two dissimilar types of energy-releasing nuclear reactions in which energy is unconfined from high-powered atomic bonds between the particles inside the nucleus. The major difference between these two process is that fission is the splitting up of a heavier nucleus into the two or more lighter nuclei while fusion is the fusing of two or more lighter the nuclei into a heavier one. The nuclear reactor is a device to initiate and control a continued nuclear chain reaction. A high amount of energy is unconfined in nuclear fission as well as in nuclear fusion. however in case of nuclear reactor it is the nuclear fission reaction which occurs. In this container, kinetic energy of the fission reaction crop finally converted into thermal energy when these nuclei collide with in close proximity atoms. The reactor absorbs some gamma rays and therefore a high amount of heat is generated in the nuclear fuel elements. This heat must be removed from the fuel and reactor core and used to create electrical power. The coolant which can be a liquid or a gas transports the heat to the heat exchanger or directly to the turbines subsequently that electricity can be produced.

II. LITERATURE REVIEW

Yamagata et al.[8] is perhaps one of the most popular dataset used for the validation of numerical models. They investigated forced-convective heat transfer to supercritical water flowing in tubes and found that for water flowing in vertical and horizontal tubes the heat transfer coefficient increases significantly in the pseudocritical region

Ornatskii et al. [15] investigated the heat transfer of water with rising and falling flow at supercritical pressures in a tube with the diameter of 3 mm

Ornatskii et al. [16] investigated the normal and the deteriorated heat transfer in a vertical annular channel (external tube heating). The deteriorated heat-transfer zone was observed visually as a red hotspot, appearing in the upper section of the test tube.

Glushchenko et al. [17] conducted experiments with an upward flow of water in vertical tubes and in vertical annular channels by means of external and internal one-side heating at supercritical pressure.

Jue Yang et al. [46] have investigated the heat transfer in upward flows of supercritical water in circular tubes and in tight fuel rod bundles is numerically using the commercial CFD code STAR-CD 3.24

S. Gao, D.C. Leslie and G.F. Hewitt [47] forms part of a research project that aims to evaluate and improve the TRAC (transient reactor analysis code) code behavior by comparing code predictions with a range of single effect experiments.

S.D. Yu and S. Xu [48] have done modeling and analysis of three-dimensional steady-state heat transfer in a CANDU nuclear fuel rod which are presented in their paper.

III. OVERVIEW OF THE CFD

The mainly fundamental consideration in the CFD to how one treats a continuous fluid in a discredited fashion on the computer. One method is to discredit the spatial domain into equations of the motion (Euler equations for inviscid and Navier-Stokes equations for viscous flow). In adding up, such a mesh can be either irregular (for illustration consisting of triangles in 2D, or pyramidal solids in 3D) or regular; the distinctive characteristic of the former is that each cell must be stored separately in the memory. It is possible to steadfastly solve the Navier- Stokes equations for laminar flows and for turbulent flows when all of the applicable length scales can be resolved by the grid (a direct

numerical simulation). In general, still, the range of length scales appropriate to the problem is larger than even today's massively parallel computers can model. In these luggage, turbulent flow simulations necessitate the introduction of a turbulence model. Large Eddy Simulations (LES) and the Reynolds-Averaged Navier-Stokes equations (RANS) formulation, with the k-ε model or the Reynolds stress model, are two techniques for selling with these scales. In many instances, other equations are solved concurrently with the Navier-Stokes equations. These other equations can embrace those describing variety concentration (mass transfer), chemical reactions, heat transfer, etc.

A. *Uses of the CFD*

The CFD is used by engineers and scientists in a wide range of the fields characteristic applications include:

- To process industry: Mixing vessels and chemical reactors
- To building services: Ventilation of buildings and atriums
- To health and safety: Investigating the effects of fire and smoke
- Motor industry: Combustion modeling and car aerodynamics
- To electronics: Heat transfer within and around circuit boards
- To environmental: Dispersion of pollutants in air or water
- To power and energy: Optimization of combustion processes
- To medical: Blood flow through grafted blood vessels

B. *Advantages of the CFD*

- It provides the flexibility to change design parameters without the expenditure of the hardware changes. It thus costs less than laboratory or field experiments.
- It has a faster gyrate time than experiments.
- It guides the engineer to the root of tribulations and is consequently well suited for troubleshooting
- Selected fluid properties and boundary conditions are specific.

IV. SOLVING THE CFD PROBLEM

The constituent that solves the CFD problem is called the Solver. It produces the compulsory results in a non-interactive batch process. The CFD problem is solved as follows

The partial differential equations are incorporated over all the control volumes in the section of interest. This is corresponding to applying a basic conservation law (for example, for mass or momentum) to each control volume. The algebraic equations are solved by iteratively. An iterative approach is necessary because of the nonlinear nature of the equations, and as the solution approaches the precise solution, it is said to converge. Each iteration an error, or remaining, is reported as a praise of the overall conservation of the flow properties. How close the final solution is to the accurate solution depends on a number of factors, together with the size and shape of the control volumes and the size of the final residuals. Complex corporeal processes, such as ignition and turbulence, are often modeled using empirical dealings. The approximations inbuilt in these models also have a say to differences between the CFD solution and the real flow. The solution process requires no user dealings and is, therefore, typically carried out as a batch process. The solver produces a results file that is then accepted to the post-processor.

1) *Governing Equations of Fluid Dynamics*

Each of the CFD software package has to produce a prophecy of the way in which a fluid will flow for a given situation. To do this the tie together must calculate numerical solutions to the equations that preside over the flow of fluids:

- To the Continuity equation,
- To the Momentum equation,
- TotheEnergyequation.

B. *Continuity Equation*

The continuity equation is basically the equation for the conservation of mass. It is consequent by the mass balance on the fluid entering and leaving a volume element taken in the flow field. The equation for the conservation of mass for three dimensional stable flows may be stated as [1]:

[Net rate of mass flow entering volume element in x direction] + [Net rate of mass flow entering volume element in y direction] + [Net rate of mass flow entering volume element in z direction] = 0 (3.1)

An incompressible fluid, the continuity equation for a steady three dimensional flow can be written as:

$$\frac{\partial U}{\partial X}+\frac{\partial V}{\partial Y}+\frac{\partial W}{\partial Z}=0 \quad (3.2)$$

C. *Momentum Equation*

[Mass] [Acceleration in i direction] = [Body forces acting in i direction] − [Pressure forces acting in i direction] + [Surface force acting in i direction] (3.3)

x momentum

$$\rho\left[u\frac{\partial u}{\partial x}+v\frac{\partial u}{\partial y}+w\frac{\partial u}{\partial z}\right]=F_x-\frac{\partial p}{\partial x}+\mu\left[\frac{\partial^2 u}{\partial x^2}+\frac{\partial^2 u}{\partial y^2}+\frac{\partial^2 u}{\partial z^2}\right] \quad (3.4)$$

y momentum

$$\rho\left[u\frac{\partial v}{\partial x}+v\frac{\partial v}{\partial y}+w\frac{\partial v}{\partial z}\right]=F_y-\frac{\partial p}{\partial y}+\mu\left[\frac{\partial^2 v}{\partial x^2}+\frac{\partial^2 v}{\partial y^2}+\frac{\partial^2 v}{\partial z^2}\right] \quad (3.5)$$

z momentum

$$\rho\left[u\frac{\partial w}{\partial x}+v\frac{\partial w}{\partial y}+w\frac{\partial w}{\partial z}\right]=F_z-\frac{\partial p}{\partial z}+\mu\left[\frac{\partial^2 w}{\partial x^2}+\frac{\partial^2 w}{\partial y^2}+\frac{\partial^2 w}{\partial z^2}\right] \quad (3.6)$$

D. *Energy Equation*

Energy is neither created nor destroyed only conserved one form to another form .The conservation of energy is derived from the first law of thermodynamics process. Temperature is the basis of heat and heat is one form of energy. The temperature distribution in the flow playing field is governed by the energy equation,

[rate of energy input due to conduction] + [rate of energy input due to workdone by conduction] + [rate of energy input due to workdone by surface stress] = [rate of increase of energy in the element] (3.7)

The energy equation for three dimensional flow of an incompressible fluid, constant property, Newtonian fluid is determined as [1]

$$\rho c_p\left[u\frac{\partial T}{\partial x}+v\frac{\partial T}{\partial y}+w\frac{\partial T}{\partial z}\right]=\lambda\left[\frac{\partial^2 T}{\partial x^2}+\frac{\partial^2 T}{\partial y^2}+\frac{\partial^2 T}{\partial z^2}\right]+\mu\phi \quad (3.8)$$

Where, the viscosity-energy-dissipation function ϕ is defined as:

$$\phi=2\left[\left(\frac{\partial u}{\partial x}\right)^2+\left(\frac{\partial v}{\partial y}\right)^2+\left(\frac{\partial w}{\partial z}\right)^2\right]+\left(\frac{\partial u}{\partial x}+\frac{\partial v}{\partial y}+\frac{\partial z}{\partial y}\right)^2 \quad (3.9)$$

1) Discretization Methods

The constancy of the chosen discretization is usually established numerically rather than analytically as with simple linear problems. Extraordinary care must also be taken to ensure that the discretization handles discontinuous solutions charmingly. The Euler equations and Navier-Stokes equations both admit shocks, and contact surfaces. Several of the discretization methods being used are discussed below

2) Finite Volume Method (FVM)

This is the "classical" or standard approach used mainly often in commercial software and research codes. The governing equations are solved on the discrete control volumes. The FVM recasts the PDE's (Partial Differential Equations) of the N-S equation in the conventional form and then discretize this equation [1].

$$\frac{\partial}{\partial t}\iiint Q\, dV + \iint F\, dA = 0 \quad (3.10)$$

3) Finite Element Method (FEM)

This method is fashionable for structural analysis of solids, but is also appropriate to fluids. The FEM formulation requires,

$$R_i = \iiint W_i Q\, dV^e \quad (3.11)$$

4) Finite Difference Method (FDM)

This method has historical significance and is simple to program. It is presently used in few specialized codes only. Modern finite difference codes make use of an entrenched boundary for handling complex geometries assembly these codes highly efficient and accurate.

V. MODELING OF THE FUEL ROD ASSEMBLY

The heat generated by the nuclear fission is conducted from beginning to end the fuel rod and then convicted to the surrounding coolant in the flow channel. The heat transfer from fuel rod to the coolant is shown in the following the Fig. 1.

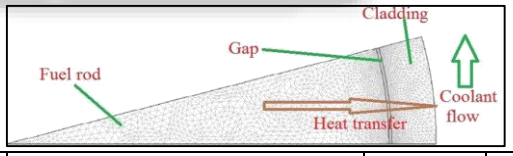

Fig. 1: The Fuel Rod Cross-Section (top view) [1]

A. Properties of the materials

The thermo physical properties of fuel pellet (UO_2)[2], cladding (stainless steel), [2] gap (He)[2] and coolant (R-12)[4] are show give below from the Table 1 to 4 respectively.

Properties	Value
Thermal Conductivity	30 W/m-K
Specific heat (c_p)	269 J/kg-K
Density	11000 kg/m^3
Poisson's Ratio	0.285
Thermal coefficient of Expansion	10.7×10-6/ºC

Table 1: Constant thermo physical properties of fuel (UO_2)

Temperature (K)	393	438	483
Pressure (MPa)	4.64	4.64	4.64
Density (kg/m^3)	541.20	218.30	171.88
Specific Volume (m^3/kg)	0.0018481	0.0045809	0.0058184
Internal energy (kJ/kg)	348.04	410.24	445.80
Enthalpy (kJ/kg)	356.68	431.55	472.74
Entropy (kJ/K)	1.4488	1.6324	1.7222
CV (J/g-K)	0.80785	0.68146	0.68943
CP (J/g-K)	8.2556	0.98535	0.87336
Sound velocity (m/s)	97.164	143.19	165.98
Viscosity (Pa-s)	0.000033340	0.000020983	0.000021935
Thermal conductivity (W/m-K)	0.040429	0.020559	0.021204
Phase	supercritical	supercritical	supercritical

Table 2: Thermo physical properties of coolant (R-12)

Sl. No	Parameter	Notation	Geometry (360^0 sector)	Geometry (sub channel 1)	Geometry (sub channel 2)
1	Hexagonal side length (mm)	S	18.3	18.3	18.3
2	Fuel rod diameter (mm)	D	9.5	9.5	9.5
3	Adiabatic wall thickness (mm)	t	0.3	0.3	0.3
4	Pitch (mm)	p	11.29	11.29	11.29
5	Heated length (mm)	L	1000	1000	1000
6	Total perimeter (mm)	Pr	318.715	16.71	42.59
7	Free flow area (mm$_2$)	A	373.89	19.77	44.5
8	Hydraulic diameter (mm)	D_e	4.69	4.73	4.18

Table 3: Physical dimension of fuel rod assembly

B. Creation of Geometries

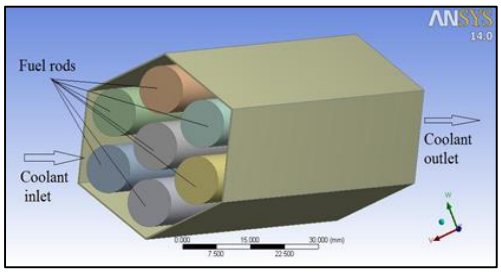

Fig. 2: Hexagonal fuel rod assembly

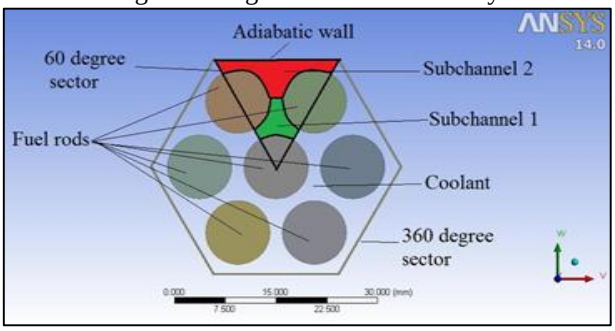

Fig. 3: the Cross section of hexagonal fuel rod assemblage

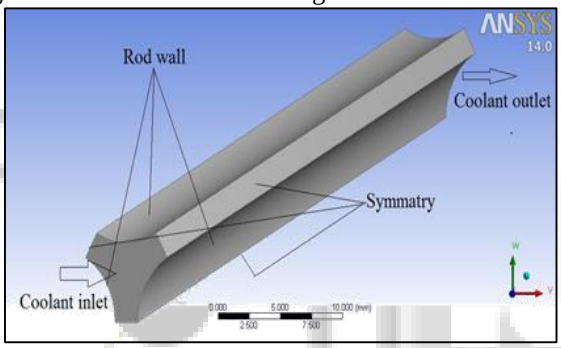

Fig. 4: to Sub channel 1 (middle sub channel)

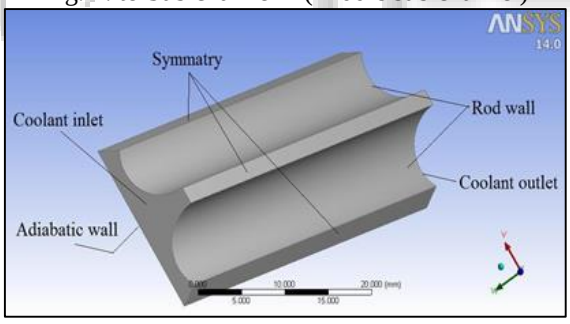

Fig. 5: Sub channel 2 (corner sub channel)

C. Meshing of Geometries

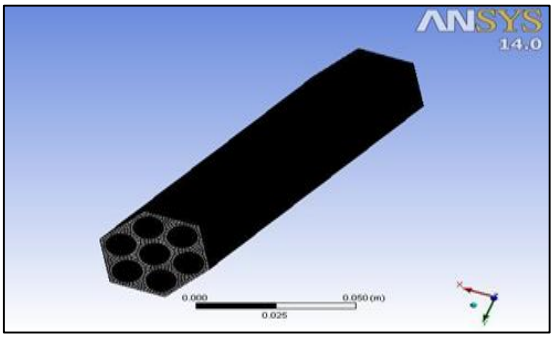

Fig. 6: Meshing of sub channel 1

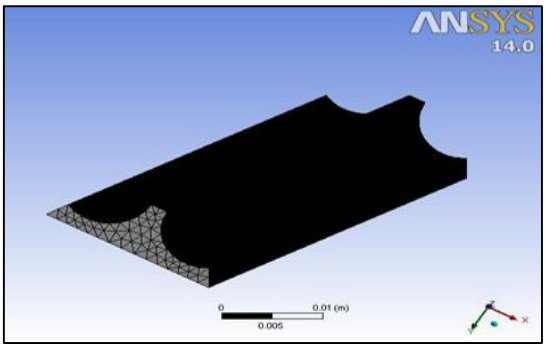

Fig. 7: Meshing of sub channel 2

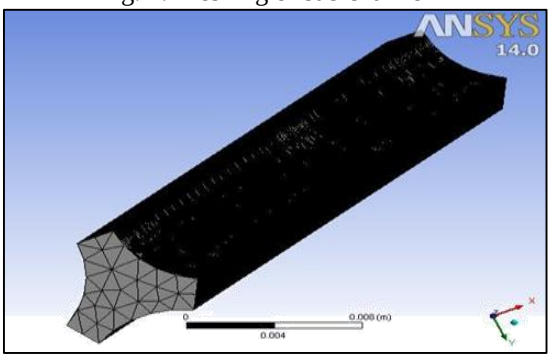

Fig. 8: Meshing of 7 fuel rod assembly

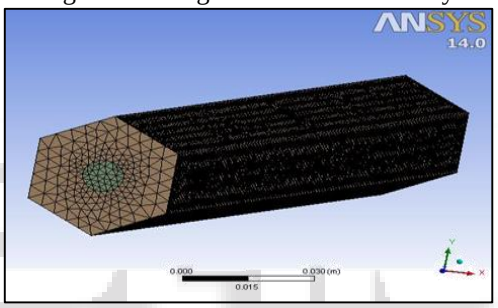

Fig. 9: Meshing of single fuel rod assembly

D. CFD Analysis

The CFD simulation is carried out in these two sub channels as well as in the preferred domain of the 7 fuel rod assemblage and single fuel rod assembly through which R-12 flows as coolant.

Serial no	Parameters	value
1	Inlet pressure	4.64 Mpa
2	Inlet temperature	393 K
3	Heat flux	33.6 kW/m^2
4	Mass flux	518 kg/m^2-s

Table 4: Different parameters used for computation

E. Accuracy of Present the CFD and Turbulence Models

To attain appropriate numerical simulation and best result from it; appropriate defining of the solver and viscous model, material properties, practical boundary conditions and solution controls are obligatory. The heat transfer to supercritical water in the cooling channels of a Supercritical Water Reactor (SCWR) has been investigated by using the CFD in numerous studies. The general governing equations which are appropriate for the simulation of flow and heat transfer with supercritical fluids are give below:

Prime: The mean values are obtained by an averaging process:

$$\bar{u}_i = \lim_{\infty} \Delta t \to \frac{1}{\Delta t} \int_t^{t+\Delta t} u_i(x,\tau)d\tau \qquad (4.6)$$

When the Favre averaging is used, it is customary to decompose the instantaneous velocity into the mass-averaged part, $\tilde{}$ and a turbulent fluctuating part, u_i , therefore,

$$u_{i=}\tilde{u_i} + u_i'' \quad (4.8)$$

1) *Continuity's*

$$\frac{\partial \bar{\rho}}{\partial t} + \frac{\partial(\bar{\rho}\widetilde{u_i})}{\partial x} = 0 \quad (4.9)$$

2) *Momentum eq^n*

$$\frac{\partial \bar{\rho}\widetilde{u_i}}{\partial t} + \frac{\partial(\bar{\rho}\widetilde{u_i}\widetilde{u_j})}{\partial x_j} = -\frac{\partial \bar{p}}{\partial x_i} + \frac{\partial}{\partial x_j}\left(\overline{\tau_{ij}} - \bar{\rho}\widetilde{u_i''u_j''}\right) + \bar{\rho}g \quad (4.10)$$

3) *Energy Equation*

$$\frac{\partial \bar{\rho}c_p\widetilde{T}}{\partial t} + \frac{\partial(\bar{\rho}c_p\widetilde{u_j}\widetilde{T})}{\partial x_j} = -\frac{\partial}{\partial x_j}\left(\lambda\frac{\partial \widetilde{T}}{\partial x_j} - \bar{\rho}c_p\widetilde{u_j''T''}\right) \quad (4.11)$$

4) *Eddy Viscosity*

$$\mu_t = \bar{\rho}c_\mu\frac{k^2}{\varepsilon} \quad (4.17)$$

5) *Turbulence Kinetic Energy*

$$\frac{\partial \bar{\rho}k}{\partial t} + \frac{\partial(\bar{\rho}\widetilde{u_j}\,k)}{\partial x_j} = \frac{\partial}{\partial x_j}\left[\left(\bar{\mu} + \frac{\mu_t}{\sigma_k}\right)\frac{\partial k}{\partial x_j}\right] + \mu_t\frac{\partial \widetilde{u_i}}{\partial x_j}\left(\frac{\partial(\widetilde{u_i})}{\partial x_j} + \frac{\partial(\widetilde{u_j})}{\partial x_i}\right) - \bar{\rho}\varepsilon \quad (4.18)$$

6) *Dissipation Rate*

$$\frac{\partial \bar{\rho}\varepsilon}{\partial t} + \frac{\partial(\bar{\rho}\widetilde{u_j}\,\varepsilon)}{\partial x_j} = \frac{\partial}{\partial x_j}\left[\left(\bar{\mu} + \frac{\mu_t}{\sigma_\varepsilon}\right)\frac{\partial \varepsilon}{\partial x_j}\right] + c_{\varepsilon_1}\frac{\varepsilon}{k}\mu_t\frac{\partial \widetilde{u_i}}{\partial x_j}\left(\frac{\partial(\widetilde{u_i})}{\partial x_j} + \frac{\partial(\widetilde{u_j})}{\partial x_i}\right) - \bar{\rho}c_{\varepsilon_2}\frac{\varepsilon^2}{k} \quad (4.19)$$

VI. RESULTS AND DISCUSSIONS

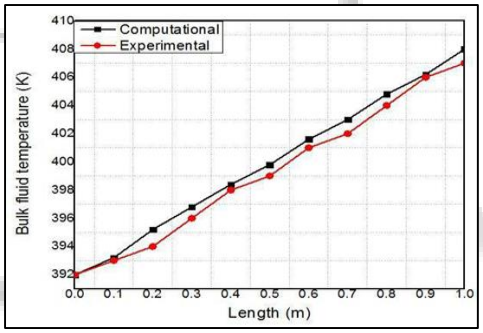

Fig. 10: to comparison between Computational as well as Experimental bulk fluid temperatures

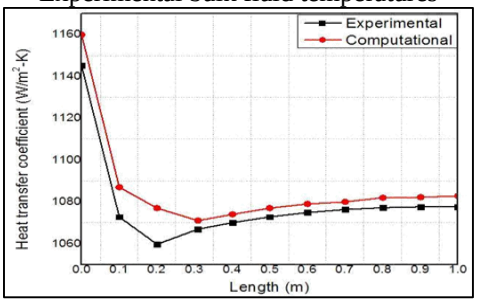

Fig. 11: to comparison between Computational as well as Experimental heat transfer coefficient

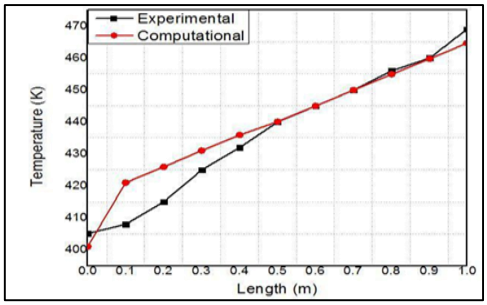

Fig. 12: to comparison between Computational as well as Experimental wall adjacent temperature

A. *Variation of Reynolds number along heated length*

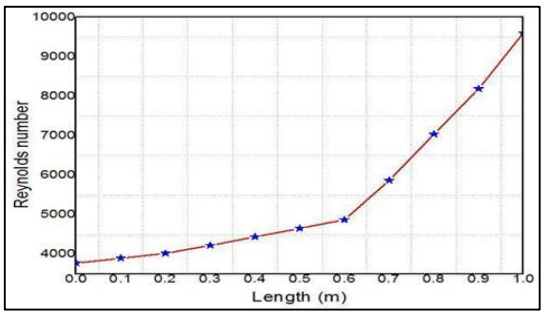

Fig. 13: Variation of Reynolds no along heated length (subchannel 1)

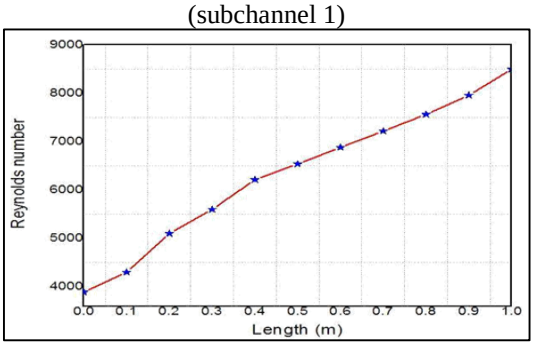

Fig. 14: Variation of Reynolds no along heated length (subchannel 2)

Reynolds number is significant in analyzing any type of flow when there is considerable velocity gradient. Usually for pipe flow, flow is deliberate to be Laminar when Re < 2300; Transitional flow when 2300 < Re > 4000 and Turbulent flow when Re > 4000.

B. *Variation of fundamental properties along the heated length*

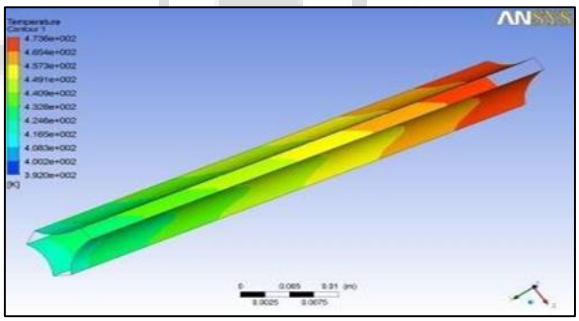

Fig. 15: Static temperature contour

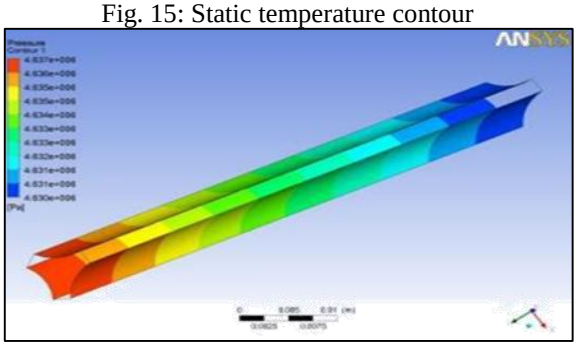

Fig. 16: Pressure contour

C. Comparison between the two subchannels

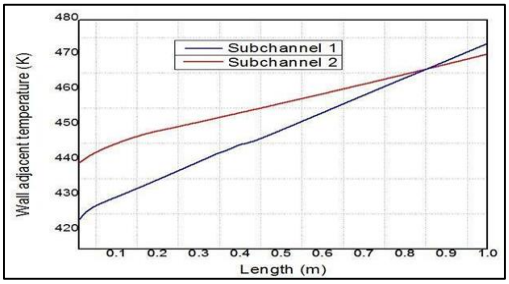

Fig. 17: Wall adjacent temperature

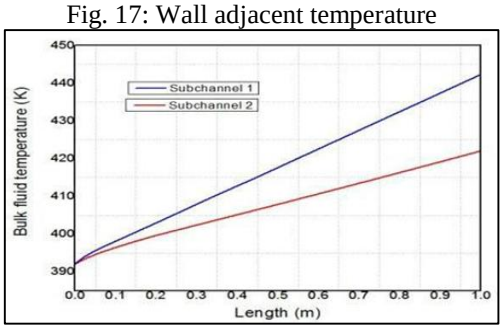

Fig. 18: Bulk fluid temperature

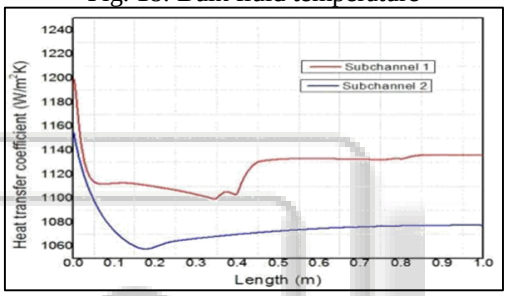

Fig. 19: Heat transfer coefficient

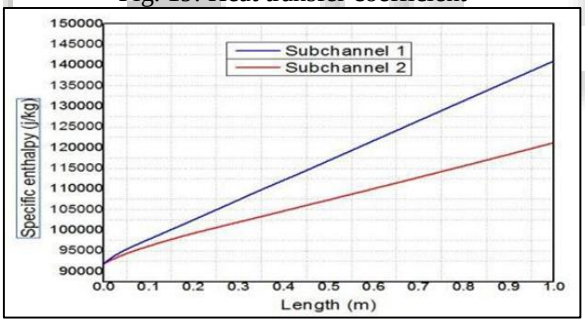

Fig. 20: Specific enthalpy

D. Hexagonal 7 rod fuel assembly

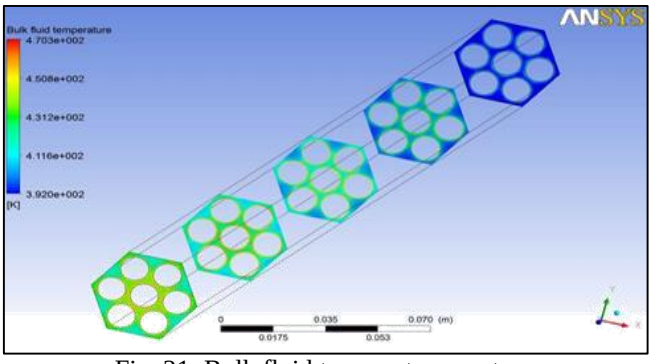

Fig. 21: Bulk fluid temperature contour

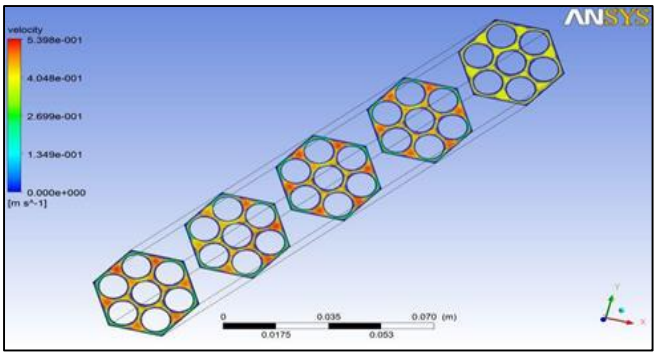

Fig. 22: Velocity contour

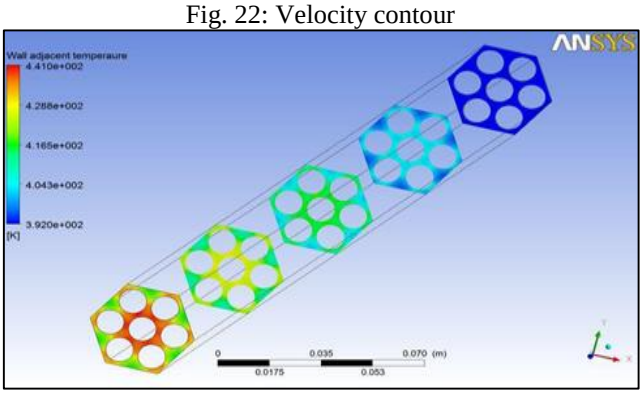

Fig. 23: Wall adjacent temperature contour

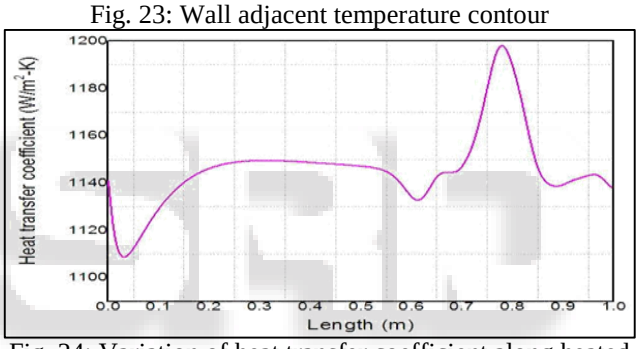

Fig. 24: Variation of heat transfer coefficient along heated length

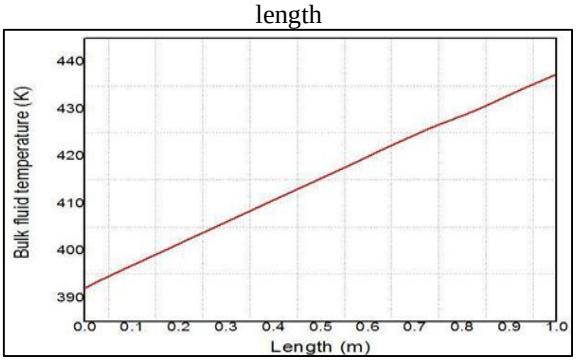

Fig. 25: Variation of bulk fluid temperature along heated length

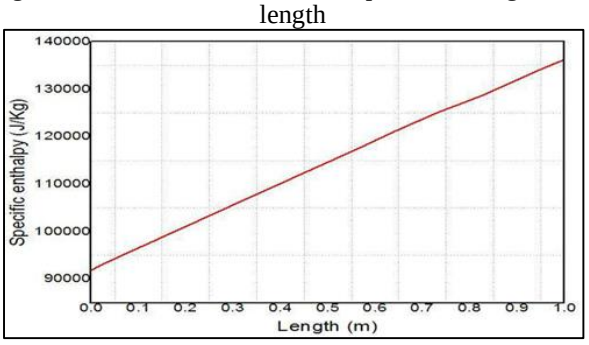

Fig. 26: Variation of specific enthalpy along heated length

VII. CONCLUSION

1) The heat transfer coefficient increases considerably but Nusselt number and Stanton number increase to some extent with the increase in R-12 mass flux while wall contiguous temperature, bulk fluid temperature and exact enthalpy decrease.
2) The heat transfer coefficient though originally decreases, once turbulence integration occurs, it increases with rising heat flux but in a lesser amount than rising with mass flux.
3) Heat transfer coefficients decreases with increase in pitch to diameter ratio. therefore for the improvement of convective heat transfer from cladding surface, pitch to diameter ratio should be decrease or for single rod assemblage, its diameter should be improved.
4) Convective heat transfer from the rod wall to the coolant is supplementary in the outer piece of the fuel rod congregation than in the middle portion.
5) With increase in the pressure; heat transfer coefficient increases considerably but at the same time bulk fluid temperature also growing with it. Hence it will not be a good idea to increase the pressure for ornamental the heat transfer coefficient for convective heat transfer from rod wall to coolant R-12. Though there must be an optimum value up to which pressure can be amplified without much rising the bulk fluid temperature.

VIII. FUTURE SCOPE

The present thesis work may be extended in the following directions,

By using singular turbulence model for different cells, one may get superior results, where heat transfer coefficient value obtained from computational consequences will be much earlier to the experimentally obtained one. To the coolant like lead and sodium can also be used in the same conditions. In this thesis; uranium di oxide is worn as fuel, in its place of uranium di oxide, liquid thorium can be used as the thorium fuel cycle have compensation over a uranium fuel cycle, counting thorium's greater abundance, concentrated plutonium and actinide production. The cladding material used in this revise is stainless steel; it can be varied with zircaloy or silicon carbide, as stainless steel has the main disadvantages of hydrogen generation.

REFERENCES

[1] A report on Nuclear Reactors generation to generations, Stephen M Goldberg and Robert Rosner, American academy of arts and sciences, October, 2010.
[2] A report on radioactive waste: production, storage and disposal, US nuclear regulatory commission, May, 2002.
[3] A report on Fundamentals of the management of radioactive waste An introduction to the management of higher-level radioactive waste on nuclear licensed sites, Guidance from the Health and Safety Executive, the Environment Agency and the Scottish Environment Protection Agency to nuclear licensees December 2007.
[4] Sarah J. Mokry, Igor L. Pioro and Romney B. Duffey ―Experimental Heat Transfer to Supercritical CO_2 Flowing Upward in a Bare Vertical Tube.‖, Proceedings of $SCCO_2$ Power Cycle Symposium 2009.
[5] Rozhgar Othman, ―Steady State and Transient Analysis of Heat Conduction in Nuclear Fuel Elements.‖, Master's Degree Project Stockholm, Sweden 2004.
[6] K. Goldmann, "Heat transfer to supercritical water at 5000 psi flowing at high mass-flow rates through round tubes," International Heat Transfer Conference, University of Colorado, Boulder, CO, USA: 1961, pp. 561-568.
[7] K. Nishikawa and K. Miyabe, "On the boiling-liking phenomena at supercritical pressures," Memoirs of Faculty of Engineering 25, Kyushu University, Japan: 1965, pp. 1-25.
[8] K. Yamagata, K. Nishikawa, S. Hasegawa, T. Fujii, and S. Yoshida, "Forced convective heat transfer to supercritical water flowing in tubes," International Journal of Heat and Mass Transfer, vol. 15, Dec. 1972, pp. 2575-2593.
[9] A. Bishop, R. Sandberg, and L. Tong, A review of heat transfer and fluid flow of water in the supercritical region and during "once-through" operation, Pittsburgh, PA, USA: Westing house Electric Corporation, Atomic Power Division, 1962.
[10] A. Bishop, R. Sandberg, and L. Tong, Forced convection heat transfer to water at near-critical temperatures and super-critical pressures, Pittsburgh, PA, USA: Westing house Electric Corporation, Atomic Power Division, 1964.
[11] E. Krasnoshchekov and V. Protopopov, "Heat transfer at supercritical region in flow of carbon dioxide and water in tubes," Thermal Engineering, vol. 12, 1959, pp. 26-30.
[12] E. Krasnoshchekov and V. Protopopov, "About heat transfer in flow of carbon dioxide and water at supercritical region of state parameters," Thermal Engineering, vol. 10,1960, p. 94.
[13] E. Krasnoshchekov, V. Protopopov, F. Van, and I. Kuraeva, "Experimental investigation of heat transfer for carbon dioxide in the supercritical region, "Proceedings of the 2nd All-Soviet Union Conference on Heat and Mass Transfer, Minsk, BSSR, 1967.
[14] E. Krasnoshchekov, V. Protopopov, I. Parkhovnik, and V. Silin, "Some results of an experimental investigation of heat transfer to carbon dioxide at supercritical pressure and temperature heads of up to 850 ºC," High Temperatures, vol. 9, 1971, pp. 992-995.

